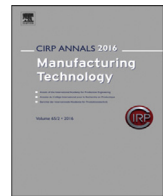




Contents lists available at ScienceDirect

CIRP Annals - Manufacturing Technology

journal homepage: <https://www.editorialmanager.com/CIRP/default.aspx>

Identification of coexisting dynamic coupling regimes in high-speed directed energy deposition

Patrick Gajek, Helena Wexel, Frederik Zanger (2)*

wbk Institute of Production Science, Karlsruhe Institute of Technology (KIT), Kaiserstraße 12, 76131 Karlsruhe, Germany

ARTICLE INFO

Article history:

Available online xxx

Keywords:

Additive manufacturing (AM)
Condition monitoring
Photometric emission

ABSTRACT

High-speed directed energy deposition (HS-DED) fundamentally alters laser–material interaction dynamics due to coexisting fast plasma-related and delayed thermal responses, complicating process stability in transition regimes. This work investigates the dynamic behavior of AISI 316 L processed on a commercial HS-DED system. It is shown that conventional grey-box models based on spatially integrated photometric signals fail to describe the process response at critical operating points. Using multispectral photometric measurements, the emission signal is temporally separated into plasma-related and thermal components. Based on this, a time-domain metric termed spectral lag is introduced, providing an emissivity-independent indicator that reliably captures regime transitions.

© 2026 The Authors. Published by Elsevier Ltd on behalf of CIRP. This is an open access article under the CC BY license (<http://creativecommons.org/licenses/by/4.0/>)

1. Introduction

High-speed laser-based directed energy deposition of metals (HS-DED-LB/M) is gaining increasing relevance in industrial applications such as repair, coating, and near-net-shape manufacturing. Compared to powder bed-based additive manufacturing processes, DED enables higher deposition rates and flexible material combinations, while HS-DED in particular allows feed rates of up to 200 *m/min* with high geometric accuracy and thermal efficiency [1], making it especially suitable for coating, functionally graded structures, and rapid repair of high-value parts. At these elevated feed rates, the laser–material interaction departs fundamentally from the conduction-dominated regime characteristic of conventional DED.

In HS-DED, a substantial fraction of the laser energy is already absorbed by the powder stream during its flight towards the substrate. As a consequence, process stability becomes highly sensitive to the balance between in-flight energy absorption and subsequent thermal coupling to the substrate and melt pool, as the process is governed by dynamic and cyclic heating and cooling behavior inherent to DED [2]. Marchese et al. [3] demonstrated that even minor variations in energy input can induce lack of fusion or porosity, underlining the critical role of thermal history in high-speed regimes. To ensure stable deposition, closed-loop process control is indispensable. The effectiveness of control strategies critically depends on an adequate representation of the underlying process dynamics. In HS-DED, these dynamics differ fundamentally from conventional DED and pose unique challenges for modelling, sensing, and control. It is emphasized that the present study is based on open-loop experiments aimed at identifying the underlying dynamic regimes and enhancing process understanding rather than implementing a closed-loop control strategy, which will be the subject of further work.

1.1. Process dynamics and control challenges

The physical difference between conventional DED and HS-DED lies in the focus and timing of energy conversion. In DED, laser energy is predominantly absorbed at the substrate surface, and the process dynamics are governed mainly by the thermal inertia of the melt pool and the surrounding material. In contrast, HS-DED operates close to a transition regime between conduction-dominated and plasma-influenced energy coupling, where both mechanisms may coexist or intermittently dominate. This results in a dual dynamic regime composed of two coupled but distinct subsystems: a fast plasma-related response in the powder stream and a delayed thermal response of the melt pool. These fundamental different time constants introduce a central control challenge. While the powder–laser interaction reacts on sub-millisecond time scales, the melt pool evolves over several milliseconds or longer. Consequently, HS-DED cannot be adequately described by a single dominant thermal time constant. Instead, the process consists of two coupled thermal systems with strongly different dynamic responses excited by the same laser input. Many existing control approaches in DED [4] represent the process as a monolithic input–output system. Linear time-invariant approximations (e.g., first- or second-order dynamics) are commonly used for conduction-dominated regimes. Their direct transfer to HS-DED is not straightforward.

While grey-box models are effective for DED control, their application to HS-DED is limited by coupled dynamics. Treating the process as a monolithic system averages out distinct powder–melt pool responses, leading to suboptimal performance. The resulting breakdown of linear models reflects a fundamental limitation rather than numerical or identification artefacts.

1.2. Photometric monitoring and signal interpretation

Photometric process monitoring is widely employed in laser-based additive manufacturing due to its high temporal resolution

* Corresponding author.

E-mail address: frederik.zanger@kit.edu (F. Zanger).

<https://doi.org/10.1016/j.cirp.2026.04.091>

0007-8506/© 2026 The Authors. Published by Elsevier Ltd on behalf of CIRP. This is an open access article under the CC BY license (<http://creativecommons.org/licenses/by/4.0/>)

and robustness. Compared to camera-based systems, photodiodes and pyrometric sensors provide bandwidths exceeding 50 kHz and are therefore well suited for HS-DED applications [5]. State of the art monitoring systems commonly combine coaxial or off-axis photometric sensing with spectral separation, where visible light spectrum (VIS) emissions are associated with plasma-related electronic transitions and near-infrared (NIR) bands are dominated by thermal radiation from the melt pool [6].

In practical HS-DED coaxial setups, the sensor field of view often captures emissions from both the powder-laser interaction zone and the melt pool simultaneously. Consequently, the measured signal represents a superposition of fast plasma-dominated and slower thermally governed emission components. For control-oriented applications, this mixed signal is typically treated as the output of a single linear time-invariant system and directly fed into grey-box models or feedback controllers [4]. While effective in stable conduction regimes, this approach becomes problematic in HS-DED transition regimes, where rapid plasma-induced signal changes may be misinterpreted as variations in melt pool temperature despite delayed thermal response.

This loss of causal interpretability is further aggravated by emissivity fluctuations and spectral crosstalk, which distort radiometric intensity measurements and obscure the underlying physics [7]. From a dynamic systems perspective, the observed behavior indicates that HS-DED cannot be represented by a single low-order transfer function, as the superposition of fast and slow dynamics introduces multiple characteristic time constants that linear control models fail to resolve. Fig. 1 schematically illustrates the HS-DED interaction zone and the resulting superposition of plasma-dominated (VIS) and thermally dominated (NIR) emissions within the sensor field of view.

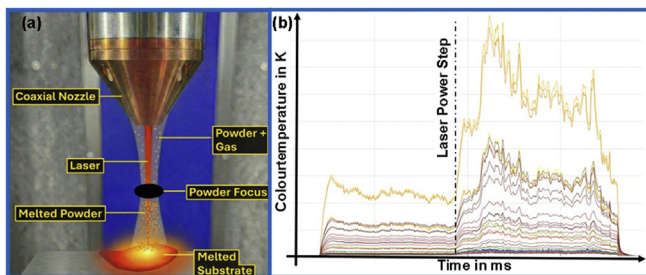


Fig. 1. HS-DED interaction zone (a) and corresponding multispectral emission signals, (b) showing the complete photometric spectrum (350–1650 nm) across all available channels.

1.3. Objective and approach

This work aims to improve process understanding and monitoring in HS-DED, where conditions are inherently non-stationary. A second-order (PT2) model based on spectrally integrated signals fails to capture the dynamics due to a temporal offset between fast plasma-related and slower thermal responses. Using spectrally resolved measurements and controlled power steps, these dynamics are separated, revealing a characteristic spectral lag between wavelength bands. Based on this time-scale separation, a time-domain metric termed spectral lag is introduced. The metric relies on relative temporal features rather than absolute signal amplitudes and is therefore robust against emissivity-induced amplitude fluctuations [3], providing a physics-based basis for monitoring and control.

2. Experimental basis and data acquisition

To enable a physically consistent analysis of spectral and temporal dynamics, the experimental setup provides controlled access to plasma and thermally dominated emission mechanisms, supporting system identification and spectral decoupling.

2.1. Experimental setup and material system

The experimental setup is based on a 5-axis PE3D system (Ponticon GmbH, Germany) operated in 3-axis mode with a stationary processing head and a moving build platform. A 6 kW LDF 6000–40 diode laser (Laserline GmbH, Germany) with a 400 μm fibre core was used, operating at a central wavelength of approximately 1080 nm, providing a top-hat intensity profile and a focus diameter of 1.0 mm. Powder was supplied coaxially through a continuous annular gap of a coaxial nozzle, using gas-atomized AISI 316 L stainless steel powder with a particle size between 20 and 63 μm (m4p material solutions GmbH, Bad Marienberg Germany).

2.2. Multispectral photometric sensing

A central deficit of conventional process monitoring is the reliance on single-channel radiometric measurements, the accuracy of which is massively compromised by fluctuating emissivity, as recently criticized by Penny et al. (2025) [7]. To overcome this limitation, a multispectral sensor (4DTWO, 4D Photonics GmbH, Germany) was integrated coaxially into the beam path. The sensor captures the photometric emissions of the process, resolving them into 32 discrete spectral channels at a sampling rate of 10 kHz. This allows for a differentiated analysis of emission sources, similar to the approach by Mafia et al. [8], who showed that synchronous monitoring of multiple melt pool descriptors is essential for stable control. The optical system uses a dichroic beam splitter to separate the back-reflection of the laser radiation (>900 nm) from the thermal process radiation. The channels are divided into the VIS range (350–900 nm), dominated by plasma transitions, and the NIR range (1000–1650 nm), dominated by the thermal Planck radiation of the heated solid and the melt pool. The sensor operates as a multi-channel photometric system without spatial resolution, capturing a spatially integrated emission signal defined by the coaxial optical setup and the movement of the build plate. The effective measurement area corresponds to the melt pool region.

3. Methodology

To analyze non-linear transition phenomena in HS-DED, a methodological framework combining control-theoretic system identification with spectrally resolved signal analysis is employed. The approach quantifies the validity limits of linear grey-box models and introduces a physics-based metric to capture the temporal decoupling of distinct emission mechanisms in the laser–material interaction zone. This is particularly relevant as existing modeling approaches either rely on simplifying physical assumptions or lack the ability to account for process variability and uncertainty, which can significantly limit predictive accuracy [9]. By explicitly incorporating spectrally resolved process signatures, the proposed framework enables a more differentiated characterization of coupled process dynamics beyond conventional monolithic representations.

3.1. Experimental procedure: step response analysis

System identification was conducted based on the system response to controlled laser power step inputs under open-loop conditions, following established step-response and time-domain identification methods as described by Ljung [10]. The laser power served as the control input, while feed rate and powder mass flow were kept constant ($v_f = 30$ m/min, $m = 32$ g/min) throughout all experiments. Each experiment consisted of a controlled laser power step from a varied initial power level to a fixed final power of 2500 W, ensuring comparable thermal boundary conditions at high power, and was repeated three times. The response time of the laser power supply is negligible compared to the observed process dynamics and can be considered instantaneous. The initial power varied between 1800 W and 2200 W in steps of 100 W. The laser power was abruptly increased to 2500 W and held constant until a quasi-stationary

emission state was reached, enabling analysis of both the transient response and steady-state behavior.

The high temporal resolution (10 kHz) enables detailed analysis of melt path dynamics. During the quasi-stationary phase, signals were segmented into non-overlapping windows for robust analysis of intermittent fluctuations.

3.2. Baseline modelling (Grey-Box PT2)

To reflect the state of the art in control-oriented process modelling, a grey-box modelling approach based on system identification was employed. In the work of Moralejo [4], the process was approximated as a static gain between laser power and melt pool width. In contrast, first- and second-order linear time-invariant systems (PT1 and PT2) are commonly used in control-oriented modelling to capture process dynamics. PT1 and PT2 denote first- and second-order linear time-invariant systems commonly used in control-oriented modelling. A spatially and spectrally aggregated photometric signal is constructed by summing all available spectral channels and used as the model output. The PT2 model was fitted to the measured step responses using a least-squares identification procedure. Model quality was assessed using the coefficient of determination R^2 , defined here as a variance-based goodness-of-fit metric,

$$R^2 = 1 - \frac{\sum (y_i - \hat{y}_i)^2}{\sum (y_i - \bar{y}_i)^2}$$

where y_i denotes the measured aggregated photometric signal, \hat{y}_i the model prediction, and \bar{y}_i the mean of the measured signal over the evaluation window. In contrast to correlation-based definitions of R^2 , which are restricted to linear relationships, this formulation evaluates how well the identified model reproduces the measured signal relative to a trivial baseline model given by the mean signal value. Consequently, negative R^2 values indicate that the fitted PT2 model performs worse than a constant mean-value approximation. It is emphasized that R^2 is not used here to assess linear correlation or to validate the linearity assumption of the underlying process. Instead, it serves as a diagnostic indicator for model mismatch, quantifying the inability of a single low-order LTI model to represent the aggregated photometric response in the HS-DED transition regime. Persistently low or negative R^2 values are therefore interpreted as evidence that the measured signal does not originate from a single dominant dynamic subsystem, but rather from the superposition of multiple processes with fundamentally different time constants.

3.3. Spectrally coexisting dynamic regime analysis

To separate fast plasma-related and delayed thermal dynamics in HS-DED, a spectrally resolved time-domain analysis is applied. Plasma-dominated optical emissions exhibit strong high-frequency fluctuations, whereas thermally dominated emissions evolve more slowly due to thermal inertia [11].

Fig. 2 shows a representative measured step response at a laser power of 2000 W, illustrating the temporal separation $\Delta\tau$ between a plasma-dominated VIS channel and a thermally dominated NIR channel.

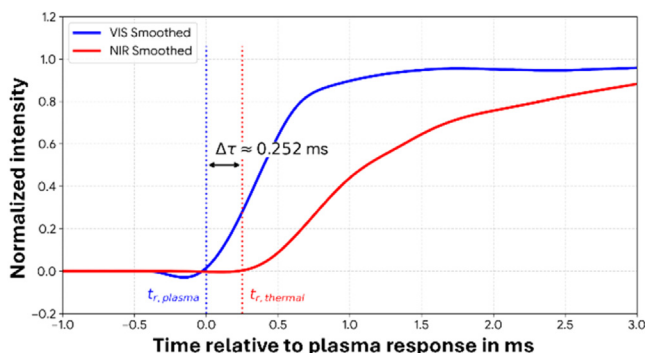


Fig. 2. Spectrally resolved step response at 2000 W, showing plasma-dominated (VIS) and thermally dominated (NIR) emissions.

The figure serves to explain the extraction of characteristic response times and is not intended as a quantitative system identification result. To obtain robust response times in the presence of plasma-induced noise, signals were normalized, smoothed, and evaluated using a threshold-based criterion. The threshold was defined as three times the baseline standard deviation, and the response time was determined as the first instance at which the signal exceeded this level with sufficient persistence. The plasma-related response time $t_{r, plasma}$ is extracted from a VIS channel dominated by electronic excitation, while the thermal response time $t_{r, thermal}$ is obtained from an NIR channel governed by Planck-like thermal radiation.

For response time extraction, a representative VIS channel at 317 nm and an NIR channel at 1017 nm were selected, based on their distinct rise-time behaviour, corresponding to plasma-dominated and thermally dominated emission, respectively. To enable direct comparison, all signals were normalized using a baseline-to-plateau scaling defined from pre-step and post-transient signal levels, rendering the transient responses independent of absolute intensity. The temporal offset between both responses defines the spectral lag:

$$\Delta\tau = t_{r, thermal} - t_{r, plasma}$$

A positive spectral lag indicates that plasma excitation precedes effective thermal coupling to the substrate. The slight undershoot observed in the smoothed VIS signal prior to the plasma response is a filtering artefact caused by the Savitzky-Golay smoothing near the step transition and has no physical significance. Later increases in the thermal signal are attributed to heat accumulation and do not affect the response time extraction. The sensitivity of the spectral lag extraction to the selected filtering parameters and threshold definition was evaluated. While absolute response times vary slightly with filter window size and threshold level, the relative temporal offset between plasma-dominated and thermal signals remains consistent. Consequently, the spectral lag is robust with respect to reasonable variations in signal processing parameters.

4. Results and discussion

The experimental analysis reveals a distinct discontinuity in the process dynamics as the laser power approaches the transition regime around 2000 W. The following sections evaluate the performance of the classical grey-box model and interpret the identified spectral coexisting dynamic regime based on the derived system parameters.

4.1. Breakdown of linear model validity

The grey-box modelling approach aims to describe the dynamic response of spatially aggregated photometric signals using a single, second-order, linear time-invariant (PT2) model. For each laser power step, a PT2 transfer function was identified from the measured step response. This was then evaluated using R^2 , a variance-based goodness-of-fit metric, to assess the fit. Across the entire high-speed operating range, the identified models exhibit consistently low or negative R^2 values, indicating a systematic model mismatch rather than isolated identification errors.

Inspection of the model residuals reveals that this mismatch originates from the inability of the PT2 model to simultaneously reproduce two distinct features of the measured response: an initially rapid signal increase immediately following the laser power step and a subsequently delayed evolution towards a quasi-stationary level. While the linear model attempts to approximate the overall trend, it cannot capture both time scales with a single set of parameters.

The aggregated photometric signal therefore reflects a superposition of fast plasma-related and slower thermally governed dynamics, violating the single-subsystem assumption underlying low-order linear time-invariant models. Consequently, the observed model breakdown is attributed to fundamental process dynamics rather than measurement noise, insufficient model order, or data quality limitations.

4.2. Distribution of spectral lag across repeated experiments

The spectral lag $\Delta\tau$, defined as the temporal offset between the plasma-related and thermal response times, was evaluated across repeated experiments to assess its robustness and sensitivity to the underlying process state. Fig. 3 summarizes the distribution of $\Delta\tau$ as a function of laser power, with each marker representing one individual experimental run performed under nominally identical conditions.

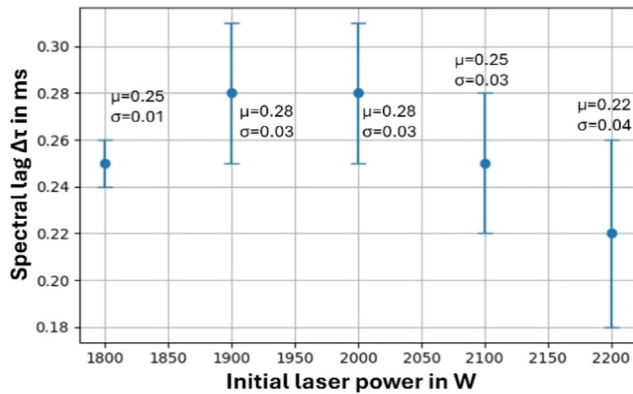


Fig. 3. Distribution of spectral lag $\Delta\tau$ versus initial laser power. Markers denote mean values (μ), error bars indicate standard deviation (σ) from repeated experiments.

The observed variations do not arise from fluctuations in laser power or traverse speed, but from changes in the effective energy coupling mechanism. Across the investigated power range from 1800 W to 2200 W, the spectral lag remains strictly positive, confirming that plasma excitation consistently precedes the thermal response of the melt pool. The magnitude of $\Delta\tau$ varies systematically between individual runs. At lower laser powers (1800–1900 W), the spectral lag exhibits a relatively narrow spread at 1800 W, followed by an increase in both mean value and variability at 1900 W. In the intermediate regime (1900–2000 W), the spectral lag reaches its highest average values ($\mu \approx 0.28$ ms) without forming a distinct peak, as similar values are observed at both power levels. This regime is characterized by increased variability compared to 1800 W, indicating enhanced sensitivity to the initial interaction state. Within this range, both weakly and strongly pronounced spectral lag values are observed under otherwise identical process parameters, suggesting the coexistence of distinct coupling states. At higher laser powers (2100–2200 W), the spectral lag decreases compared to the intermediate regime, while maintaining a comparable level of statistical variation. This trend suggests a shift towards more consistent interaction conditions, where either enhanced in-flight energy absorption or increased thermal input to the substrate reduces the temporal decoupling between plasma and melt pool dynamics. As such, the spectral lag captures subtle differences in process state that remain hidden in spatially integrated intensity signals. The consistency of the observed trends across repeated experiments supports the robustness of the identified process behavior. The present study demonstrates that $\Delta\tau$ is a sensitive and reproducible metric for characterising the degree of temporal decoupling in HS-DED. The systematic variation of the process across repeated experiments provides direct evidence that the process cannot be described by a single, unique dynamic state. This in turn motivates the regime-based interpretation discussed in the following section.

4.3. Physical interpretation of the spectral lag

The interpretation of plasma-dominated and thermal regimes is based on spectrally separated photometric emissions and is not supported by independent diagnostics. The variation of spectral lag reflects changes in the dominant energy coupling mechanisms in HS-DED. Small spectral lag values indicate tightly coupled plasma excitation and thermal response. In this regime, stable melt pool formation

is primarily driven by direct laser–substrate interaction, while plasma and powder-related emissions primarily reflect process conditions, as laser–powder interactions lead to attenuation and redistribution of the incident energy before reaching the substrate [12].

In contrast, larger spectral lag values indicate a pronounced temporal decoupling between plasma excitation and thermal response, where plasma-related electronic excitation responds almost instantaneously to laser power changes while the thermal response of the melt pool is delayed. This temporal offset reflects fundamentally different characteristic time scales, with sub-millisecond plasma dynamics and slower millisecond-scale thermal responses. This behavior is consistent with plasma-dominated interaction regimes, in which increased in-flight absorption, plasma shielding, or partial decoupling of energy transfer reduce the effective thermal input to the substrate [11,13]. The coexistence of weakly and strongly pronounced spectral lag values under nominally identical process conditions suggests intermittent switching between these interaction regimes, as previously reported for laser-based manufacturing processes operating near stability limits [14].

In such regimes, a single characteristic time constant or steady-state representation is insufficient. The spectral lag enables the distinction between process states with similar integrated intensity but fundamentally different dynamic coupling behavior. It further explains the limited performance of conventional control approaches, as aggregated signals combine fast plasma-related and delayed thermal dynamics, leading to conflicting and partially non-causal control-relevant information. Consequently, control actions may be driven by plasma-induced variations that are not representative of the melt pool state. The spectral lag is therefore not a direct control variable, but a physically interpretable indicator of regimes where conventional linear control models are no longer valid.

5. Conclusion and outlook

This study demonstrates that high-speed directed energy deposition exhibits coexisting dynamic regimes that cannot be captured by conventional linear grey-box models. Open-loop step response analysis reveals a breakdown of PT2 model validity in the transition regime due to the superposition of fast plasma-related and delayed thermal dynamics. Using spectrally resolved photometric measurements, these dynamics are separated and quantified by the spectral lag $\Delta\tau$, defined as the temporal offset between plasma excitation and thermal response. $\Delta\tau$ exhibits reproducible, power-dependent behavior across repeated experiments, with variations remaining within a well-defined statistical range. This consistent behavior indicates the presence of multiple, physically distinct process states and suggests intermittent transitions between different energy coupling regimes. As a relative time-domain metric, $\Delta\tau$ is robust against emissivity-related distortions and reveals process state information not accessible through intensity-based monitoring. Future work will address real-time regime detection and transfer to other materials. The results provide a basis for hybrid modelling of regime-dependent dynamics.

Declaration of competing interest

The authors declare that they have no known competing financial interests or personal relationships that could have appeared to influence the work reported in this paper.

CRediT authorship contribution statement

Patrick Gajek: Writing – original draft, Visualization, Validation, Project administration, Methodology, Investigation, Data curation, Conceptualization. **Helena Wexel:** Writing – review & editing, Validation, Project administration, Funding acquisition. **Frederik Zanger (2):** Writing – review & editing, Validation, Supervision, Resources, Funding acquisition, Conceptualization.

References

- [1] Schopphoven T, Gasser A, Wissenbach K, Poprawe R (2016) Investigations on Ultra-High-Speed Laser Material Deposition as Alternative for Hard Chrome Plating and Thermal Spraying. *Journal of Laser Applications* 28(2):022501. <https://doi.org/10.2351/1.4943910>.
- [2] Yang S, Clare AT, Bennett C, Jin X (2024) Informing Directed Energy Deposition Strategies Through Understanding the Evolution of Residual Stress. *Additive Manufacturing* 79:103907. <https://doi.org/10.1016/j.addma.2023.103907>.
- [3] Marchese G, et al. (2017) Characterization and Comparison of Inconel 625 Processed by Selective Laser Melting and Laser Metal Deposition. *Advanced Engineering Materials* 19(3):1600635. <https://doi.org/10.1002/adem.201600635>.
- [4] Moralejo S, et al. (2017) A Feedforward Controller for Tuning Laser Cladding Melt Pool Geometry in Real Time. *The International Journal, Advanced Manufacturing Technology* 89(1–4):821–831. <https://doi.org/10.1007/s00170-016-9138-7>.
- [5] Liu Y, et al. (2025) Monitoring and Control of the Direct Energy Deposition (DED) Additive Manufacturing Process Using Deep Learning Techniques: A Review. *Materials (Basel, Switzerland)* 19(1):89. <https://doi.org/10.3390/ma19010089>.
- [6] Latte M (2023) In Process Monitoring of Geometrical Characteristics in Laser Metal Deposition: A Comparative Study. presented at the *Material Forming*, 101–110. <https://doi.org/10.21741/9781644902479-12>.
- [7] R.W. Penny and A.J. Hart, "Radiometric Temperature Measurement for Metal Additive Manufacturing via Temperature Emissivity Separation," 2025, *arXiv:2502.08088*. doi: 10.48550/arXiv.2502.08088.
- [8] Maffia S, Furlan V, Previtali B (2023) Coaxial and Synchronous Monitoring of Molten Pool Height, Area, and Temperature in Laser Metal Deposition. *Optics and Laser Technology* 163:109395. <https://doi.org/10.1016/j.optlastec.2023.109395>.
- [9] Hermann F, Michalowski A, Brünnette T, Reimann P, Vogt S, Graf T (2023) Data-Driven Prediction and Uncertainty Quantification of Process Parameters for Directed Energy Deposition. *Materials (Basel, Switzerland)* 16(23):7308. <https://doi.org/10.3390/ma16237308>.
- [10] Ljung L (1999) *System Identification: Theory for the User*, 2nd ed. Prentice HallUpper Saddle River, NJ, USA.
- [11] Fang J, Li L, Chen Y, Wu L (2005) Wavelet Analysis of Plasma Optical Signals at Pool Penetration in Laser Welding. in Mu G, Yu FTS, Jutamulia S, (Eds.) presented at the *Photonics Asia 2004*, Beijing, China403. <https://doi.org/10.1117/12.575353>.
- [12] Pinkerton AJ (2015) Advances in the Modeling of Laser Direct Metal Deposition. *Journal of Laser Applications* 27(S1):S15001. <https://doi.org/10.2351/1.4815992>.
- [13] Sibillano T, Ancona A, Rizzi D, Lupo V, Tricarico L, Lugarà PM (2010) Plasma Plume Oscillations Monitoring during Laser Welding of Stainless Steel by Discrete Wavelet Transform Application. *Sensors* 10(4):3549–3561. <https://doi.org/10.3390/s100403549>.
- [14] Zavalov YN, Dubrov AV (2021) Short Time Correlation Analysis of Melt Pool Behavior in Laser Metal Deposition Using Coaxial Optical Monitoring. *Sensors* 21(24):8402. <https://doi.org/10.3390/s21248402>.